NAZARBAYEV UNIVERSITY

School of Engineering and Digital Sciences

Bachelor of Engineering in
Mechanical and Aerospace Engineering

Design of Sustainable Dryer with Experimental and Numerical Approach

by

Kairat Galibek
Aruzhan Toleubay
Meiirzhan Yerulan

Principal Supervisor: Yerbol Sarbassov
Co-supervisor: Sergey Spotar

April 2025

Declaration

We hereby declare that this report entitled “Design of sustainable dryer with experimental and numerical approach” is the result of our project work, except for quotations and citations duly acknowledged. We also declare that it has not been previously or concurrently submitted for any other degree at Nazarbayev University.

Names: Kairat Galibek, Aruzhan Toleubay, Meiirzhan Yerulan

Date: April 30, 2025

Acknowledgments

We sincerely thank the School of Engineering and Digital Sciences of Nazarbayev University for providing the facilities and resources required to conduct this capstone project.

Special thanks to Professor Yerbol Sarbassov for his invaluable guidance and support throughout the entire project.

Also, we would like to sincerely thank Professor Sergey Spotar for his supervision and advice in modeling, design and materials.

Abstract

The capstone project focuses on designing a small-scale sustainable drying unit to study the drying process of wet materials under relatively dry air applicable for the subcontinental climate of the Astana region. This project explores the design, performance, and sustainable drying processes of wet materials, with a focus on waste coffee grounds (SCG), silica gel, and grapes under forced convection and a heater. Drying is an important process both in the waste management and food preservation industry, particularly in regions with colder weather conditions. This project simulates primarily solar greenhouse drying systems (SGHDs) typically used in warm climates and proposes a modified solar drying unit with integrated heating for colder environments. Experimental analysis was conducted in a small-scale 30 cm by 30 cm dryer. In addition, computational fluid dynamics (CFD) simulations were performed using COMSOL Multiphysics by modeling mass and heat transfer, revealing airflow dynamics and temperature distribution within the drying systems. Results demonstrated that forced convection along with a bottom heater showed the highest moisture removal rate for all tested materials, closely aligning with simulated outcomes, with an average discrepancy up to 15%. This study contributes to the development of innovative, sustainable drying technologies that reduce energy consumption, mitigate greenhouse gas (GHG) emissions, and improve operational efficiency in diverse climatic conditions. The results provide possibilities for scaling up solar drying systems in various industries such as waste management and agricultural applications, by promoting circular economy initiatives.

Table of contents

1 Introduction and Problem Statement

Drying is a process in which the water content of a certain product is decreased via transmission of water from the inner product to the surface, for it to be evaporated. In other words, drying is a procedure for moisture removal from material (Ekechukwu, 1999). Nowadays, it is a crucial method for preserving crops and is widely used across various industries, including textile manufacturing, dairy processing, cement production, clay brick and tile manufacturing, wood and timber processing, wastewater management, and biomass treatment (Pirasteh et al., 2014). The energy demand for drying processes is a significant contributor to industrial energy consumption, with drying accounting for up to 70% of the total energy use in the production of wood products, around 50% in textile fabric manufacturing, 27% in paper production, and 33% in pulp processing (Kudra, 2004). Traditional drying methods that rely on electric energy or fossil fuels consume excessive energy and emit significant GHGs (Ibrahim et al, 2024). This capstone study mainly focuses on drying spent coffee grounds, silica gel, and grapes which are relevant to waste management, recycling, and food industries. These materials were selected for their relevance to sustainability and practical applications.

Kazakhstan experiences a subcontinental and dry climate, with hot temperatures in the summer and cold temperatures in the winter (Nyssanbayeva et al., 2019). This creates a significant opportunity for drying processes, offering the potential to develop and implement efficient drying technologies that can work under special climate conditions. Astana endures a heating season that extends over six months annually, with a total of 5472°C Heating Degree Days each year. The average temperature drops to -14.2°C in January and climbs to 20.8°C in June (Kerimray et al., 2018).

Due to Kazakhstan's extreme continental climate, the outdoor relative humidity ranges from 53% in June to 80% in November (Astana Weather, n.d). Whereas, the typical indoor air humidity ranges from about 15% to 25%, as observed during the dehydration experiments where the drying of fresh apple rings was conducted under these conditions: 25°C - 27°C temperature, and 18% - 22% humidity. (Spotar et al., 2020). The abundant availability of dry air presents an opportunity to take advantage of this environment by utilizing the convective drying process. Moreover, this project examines how the combination of low indoor humidity and extreme temperature fluctuations can influence drying efficiency.

Currently, the drying of wet materials in such a climate is not widely practiced and is

inefficient, the convective dehydration process has several disadvantages, such as prolonged drying times, reduced efficiency, and poor thermal conductivity. resulting in increased (Sivakumar et al., 2016). Existing drying technologies are either inadequately optimized for extreme environmental conditions or heavily reliant on energy-intensive methodologies, which are not sustainable in the long term due to their high operational costs and inefficiency in maintaining consistent drying performance under variable atmospheric parameters. Moreover, the drying of materials such as spent coffee grounds, silica gel, and grapes requires the development of specialized systems that can operate effectively.

This project investigates the potential of solar drying systems, enhanced with supplementary heating, to function efficiently even in colder environments, with the ultimate goal of creating adaptable and sustainable drying systems. To achieve these objectives, the project designs a solar drying unit with a heating system that can operate in cold temperatures without phase changes, examining the relationship between drying rate, temperature, and humidity. The results from drying experiments will be supported by CFD simulations in COMSOL Multiphysics 6.2 to model heat and mass transfer. The study will conclude with an economic analysis, projecting small-scale experimental results to large-scale applications such as wastewater treatment plants (WWTPs). This comprehensive approach aims to optimize drying technologies and promote their application in diverse climatic conditions, providing both environmental and economic benefits.

Solar drying techniques have been enhanced throughout the years depending on advancements in materials science, innovative designs, and the integration of energy storage systems (Pandey, 2024). This project focuses on designing the sustainability of drying processes in different temperature regimes, especially in room conditions. We will examine the drying performance of wet materials, comparing results from a solar greenhouse system in large scale outdoor environments with drying processes in indoor conditions. The findings aim to inform the development of energy-efficient, sustainable drying technologies adaptable to diverse climatic challenges. We will create a drying unit with a heating system that will operate sustainably and find the dependencies between drying rate, mass change, and moisture removal. Finally, we will provide an economic analysis by projecting small-scale experiment results into large-scale dryers.

Contribution

Kairat Galibek contributed to the introduction, drying experiments, literature review, and methodology.

Aruzhan Toleubay contributed to the abstract, introduction, literature review, methodology, CFD modeling, results, experiments, and visualization.

Meiirzhan Yerulan contributed to the conclusion, literature review, methodology, simulation CFD modeling, and experiments.

2 Literature Review

2.1 Drying methods in industry

The range of industries that utilize the drying process varies from food production to mineral processing. In addition to drying as a mandatory step in the processing chain, lowering the moisture content of materials can add incidental positive effects on the whole production process. For example, dry materials weighing less are easier to transport and store (Mujumdar & Devahastin, 2000).

It is important to define that drying in the context of this work is the process of evaporation with heat applied. Therefore, processes that lower the moisture content of substances mechanically (centrifugation, filtration, etc) or use other substances such as gels (adsorption) are out of the scope of this research. Unavoidable use of heat makes drying the most energy-demanding process in the industry. The high latent heat of water changing to the vapour state and the low efficiency of heated air as a drying medium are what demand such high energy consumption. According to Mujumdar (2000), research relying on different studies, energy consumption of drying in industrial processes ranges between 10 and 25 % of the whole energy consumption during processing. Consequently, developing and integrating many sustainable drying apparatuses will be beneficial from both economic and environmental points of view.

The most common methods for drying in industries include hot air dryers, convection ovens, and tunnel dryers. A combined infrared and hot air dryer can be seen in Figure 1. These methods are classified under “hot drying”, as they operate above 80°C (Mujumdar, 2015). A large shortcoming of these methods includes their high energy consumption, risks of overheating sensitive products, and thermal damage. For example, in the food industry, high temperature drying has the effect of degrading vitamins, changing flavor, and adversely affecting the texture (Ratti, 2001). To meet these demands, many industries are now switching to low-temperature drying with dehumidified air. These dehumidified-air dryers (or desiccant dryers) remove moisture from air before it makes contact with the product, which enables effective and efficient drying at lower temperatures, below 50-60°C. Customary in the food and pharmaceutical industries, this method of drying is rapidly gaining popularity in electronics manufacturing as well. An example is freeze drying or lyophilization, which is standard in the pharmaceutical industry but requires extremely lower than freezing temperatures and operates under a vacuum (Schneid et al., 2025). For more

robust non-heat-sensitive products, circulating very dry air at 30-50°C achieves the same goal of lowering moisture removal without the need for increased energy consumption.

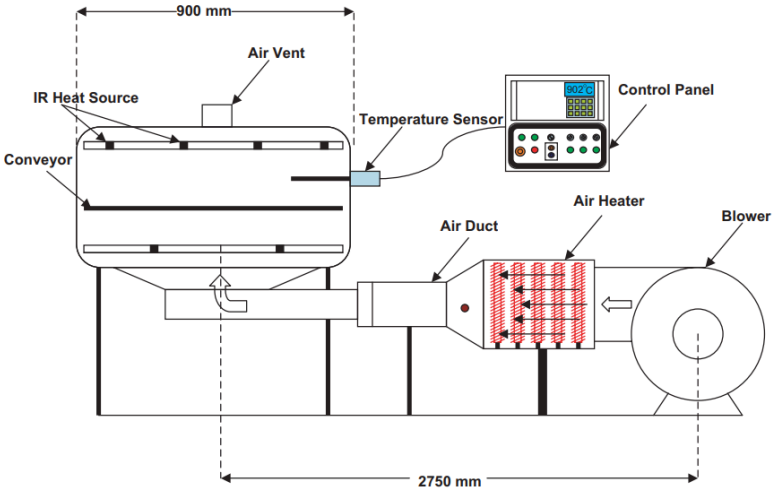

Figure 1. Combined infrared and hot air dryer (Hebbar et al., 2004)

The method of drying that is gaining more attention in recent years is solar drying, as the environmental concerns around the usage of conventional fuel are rising (Kamarulzaman et al., 2021). Multiple studies have delivered a comprehensive analysis of solar dryers' design and types. Researchers identify three types of solar dryers: direct, indirect, and hybrid (Kumar et al., 2015). When the solar radiation reaches the materials that are being dried, the solar dryer is direct. The material is placed inside the drying chamber and is directly exposed to solar radiation, see Figure 2. However, the quality of the material placed inside the direct dryer might deteriorate as a result of insufficient drying or overheating (Kamarulzaman et al., 2021). The solar dryer that uses a solar collector that heats the surrounding air is called an indirect solar dryer. The drying chamber is made of an opaque cover to prevent direct sunlight exposure, see Figure 3 (Musembi et al., 2016). Kumar et al. (2015) concluded that the indirect solar dryers that utilize forced convection display high drying speed while retaining good material properties. A hybrid solar dryer uses additional sources of energy that aid the drying process or thermal storage.

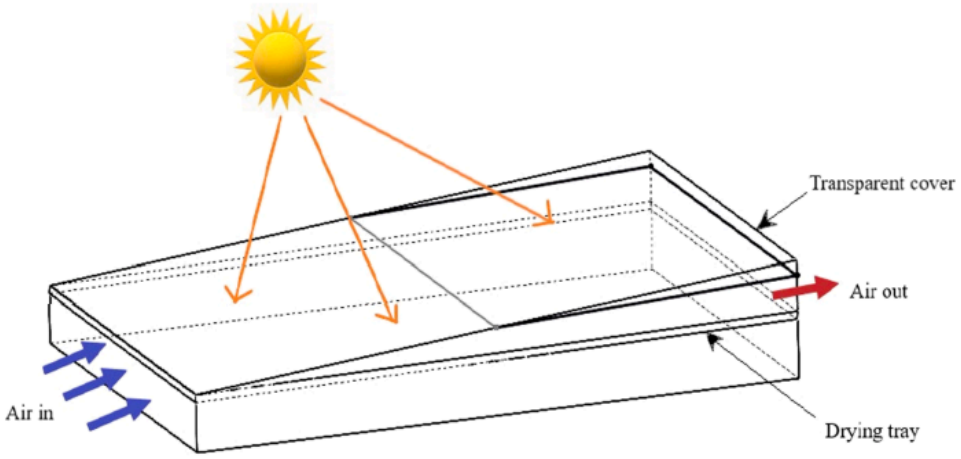

Figure 2. Direct solar dryer (Kumar et al., 2015)

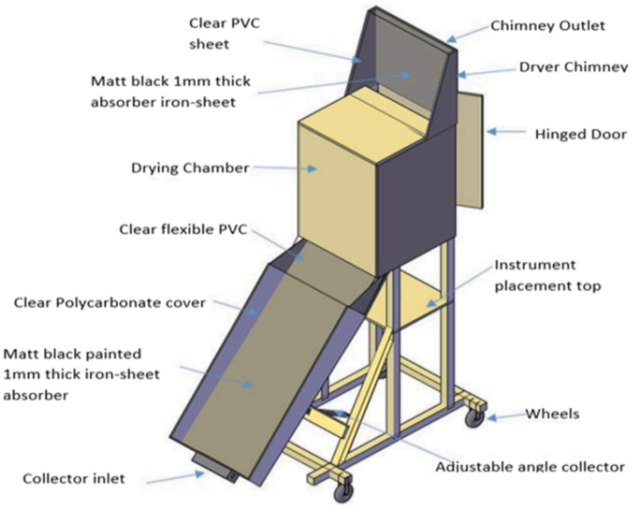

Figure 3. Indirect solar dryer (Musembi et al., 2016)

One of the recent advancements in solar drying systems is the development of flat plate-based solar dryers. Flat plate collectors can harvest both direct and diffuse solar radiation (Kumar et al.,2019). They are simple to construct, reliable, and durable, and are the most widely used solar dryers with adequate efficiency. However, high heat dissipation and poor hydraulic resistance are attributed as the main drawbacks of flat plate collectors (Kamarulzaman et al., 2021).

Evacuated Tube Collectors (ETCs) are an advanced and efficient technology used in solar drying systems, offering significant advantages in harnessing solar energy (Mevada et al., 2022). ETC-based solar dryers consist of multiple glass tubes with vacuum insulation, which minimizes heat loss and allows for efficient energy absorption even in low ambient temperatures (Pandey, 2024). The inner tubes are coated with a selective material to

maximize solar radiation absorption while reducing infrared emission. This design enables ETCs to achieve higher operating temperatures compared to flat plate or unglazed collectors, making them particularly effective for drying applications that require consistent heat. In solar dryers, ETCs are used to heat air or water, which is then circulated through the drying chamber to remove moisture from materials. Their efficiency and ability to maintain performance under diffuse sunlight make ETC-based solar dryers suitable for diverse climatic conditions, including colder regions. These systems not only reduce dependency on conventional energy sources but also improve drying rates, product quality, and energy efficiency.

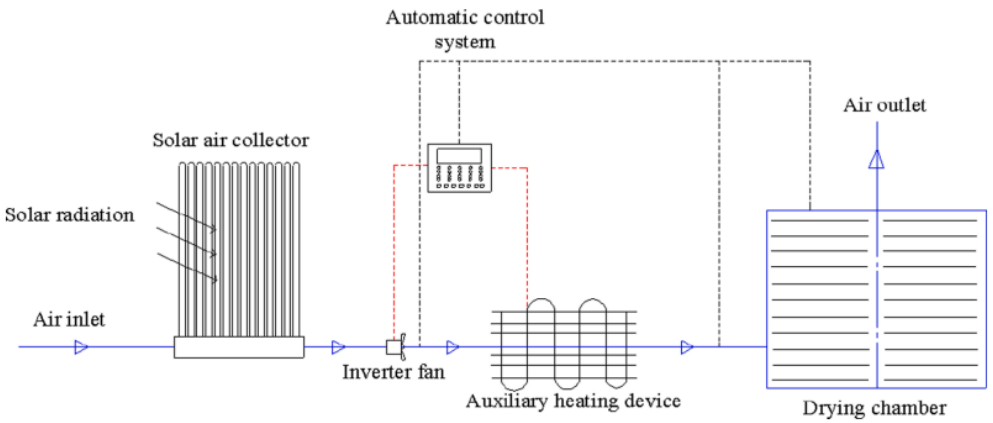

Figure 4. The ETC-based solar drying system (Wang et al., 2018)

2.2 Material Selection

2.2.1 Spent Coffee Grounds

Coffee is one of the most popular beverages in the world, with consumption rates of 2.25 billion cups per day, according to the International Coffee Organization. The trend of increasing coffee popularity and demand is also present in Kazakhstan, as overall imports of coffee nearly doubled in four years between 2019 and 2023 (Markova, 2025). An increase in coffee consumption leads to an increase in coffee production byproducts. Namely, solid residues called Spent Coffee Grounds (SCG). SCG has high potential for valorization and recycling, with a surge of research and scientific articles regarding potential uses of spent coffee grounds in the last 10-15 years (Kourmentza et al., 2018). Those uses include the creation of both biodiesel and bio-syngas, the generation of electricity, the synthesis of composites, and soil enrichment. All those prospects of SCG recycling include the important step of drying wet coffee grounds. According to Tun, dry spent coffee grounds have a longer

storage time due to limiting the growth of microorganisms such as moulds, fungi, and bacteria, which are common in coffee grounds as a result of elevated content of simple carbohydrates (Tun et al., 2020). Therefore, testing the effectiveness of a proposed dryer on SCG is important from both points of waste management and fulfilling the recycling potential of coffee grounds.

2.2.2 Floral Foam

Known in civil use as floral foam, phenol formaldehyde foam is a plastic foam used mostly in floral applications due to its high water absorption capacity (DSouza et al., 2023). The different nature of floral foam in comparison with coffee grounds, appearing in a uniform, foamy, and inorganic nature, was a reason to conduct experiments on the floral foam, testing the drying capabilities of a dryer for two different materials.

2.2.3 Silica Gel

Silica gel is a porous, amorphous form of silicon dioxide (SiO2) known and used for its moisture absorption capability. Due to its amorphous and porous nature, silica gel is capable of absorbing water up to 40% of its initial weight (Karamanis, 2015, Chapter 10). Those properties are the reason why silica gel is so widely used in industry as a vital tool to regulate humidity, preventing moisture condensation, which may lead to the spoilage of consumer goods or corrosion.

In addition to its effective moisture absorption, silica gel is a common choice due to its regenerative properties. The typical process used for removing moisture from silica gel is oven drying. Silica gel placed in an oven at temperatures between 120℃ and 140℃ for 1-2 hours restores its absorbing capabilities (Stream Peak International, 2023). However, there is a possibility to regenerate silica gel at much lower temperatures. Study by Pramuang & Exell (2007) suggests that possible regeneration temperature is as low as 40℃ if an airflow of 0.03 kg/s is present. Proving this will depict the viability of using the proposed design for the goals of regenerating silica gel, which is demanded in many industries (food, electrical, textile).

3 Methodology

Moisture content on a wet basis and drying rate were calculated from the measured mass using the following formulas (*Wet Basis*, n.d) (Ameri et al., 2019).

$$MC_{wb} = \frac{Mass\ of\ water}{Total\ mass} \quad (1)$$

$$DR = \frac{M_t - M_{t+dt}}{dt} \quad (2)$$

Where MC_{wb} is the moisture content on a wet basis, DR is the drying rate, M_t is the moisture content at the given time, M_{t+dt} is the moisture content at the next measured time, and dt is the time difference between the two measurements.

3.1 Experimental Setup

A cubic dryer was built for the experiment. The dimensions of the dryer are 30 cm in height, 29 cm in width, and 29 cm in depth, see Figure 1. The dryer was built in a cubic shape that might not appear as the most efficient shape, compared to more conventionally used cylindrical dryers (Sharma et al., 2022), but offers significantly less complex construction compared to other shapes. The dryer construction process began by assembling the wooden frame with the needed dimensions. Then, cardboard was used to cover the wooden frame and act as the walls of the dryer. Wood and cardboard were chosen due to accessibility, light weight, recyclability, and simplicity of construction using these materials. Wooden ledges on the walls inside the dryer were installed to allow drying at different heights, not only on the floor of the dryer. A heating plastic sheet was used as the floor of the dryer. It can generate 30W of heat and reach 40℃ temperature. This piece is important because heat is the mechanism through which conventional dryers dry wet materials (Goh et al., 2011), and by incorporating heat generator into the dryer design it is possible to both compare the efficiency of the fan based approach with heat based approach and analyze the efficiency of the dryer that uses both. The top of the dryer was not sealed, so that wet materials could be placed inside the dryer, but it was covered with a transparent polymer sheet. The transparent polymer sheet was pierced with an awl to create multiple holes, which can be seen in Figures 2 and 3. These holes would be the outlet, allowing the air inside to flow out of the dryer. To allow the fast air flow inside the dryer, the holes need to cover a significant amount of the surface area at the top. For this dryer, the area covered by holes is approximately 40% of the total surface area. Additionally, it was decided to make multiple small holes inside a small number of big holes to allow the air inside the dryer to circulate, which is less prone to happen if there is a big outlet through which the air can easily escape. The walls of the dryer that are parallel to each other were cut to install the fans. The fans created the airflow directed inside the dryer. Given the fact that two fans created airflow parallel to each other but were located at the opposite corners of the dryer, the purpose was to generate dry helical airflow that would accelerate the drying process.

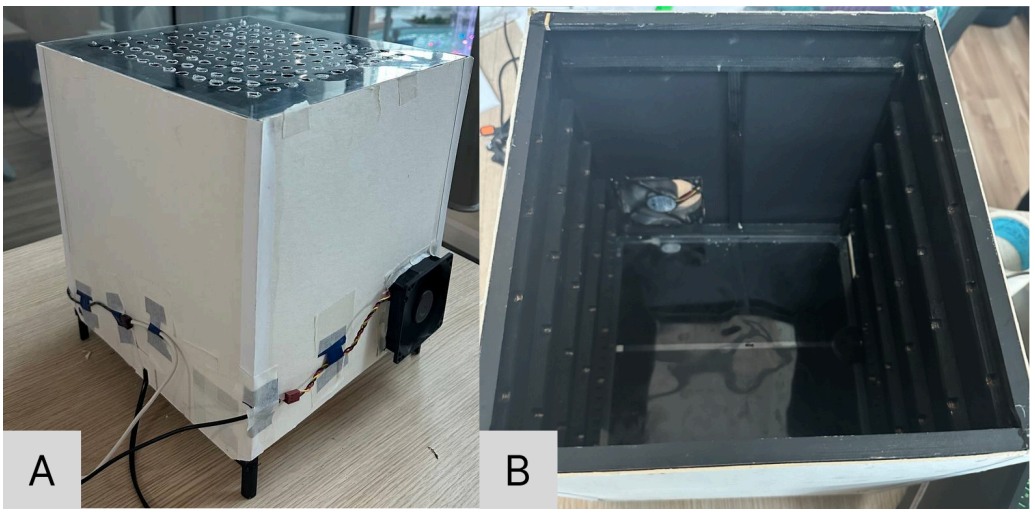

Figure 5. Experimental dryer: A - outside, B - inside

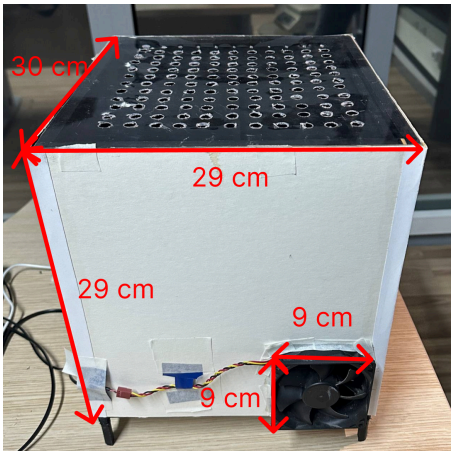

Figure 6. Dryer dimensions

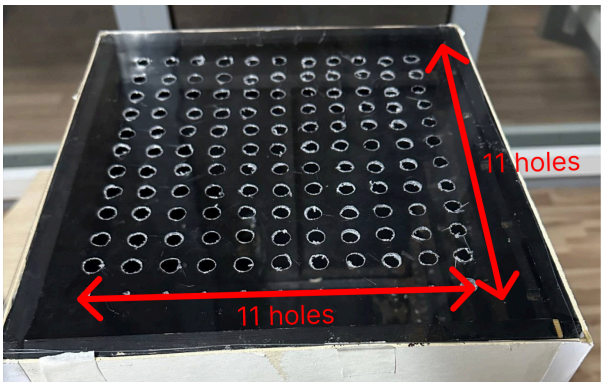

Figure 7. Top of the dryer

Figures 5, 6, and 7 show different views and dimensions of the experimental dryer used in the capstone project. Figure 5 presents two images: A – shows the external view of the dryer, while B – shows the internal structure and sample placement. Figure 6 illustrates the dimensions of the dryer, with measurements of 29 cm in height, 29 cm in width, and 29 cm in length. Two 9 by 9 cm fans are located in mirrored locations of the dryer in the corner (see Figure 6.) Figure 7 focuses on the top of the dryer, where it shows a grid of 11 holes on each side, which makes 121 outlet holes. This is a part of the outflow system designed to evenly distribute air inside the dryer for efficient drying.

3.2 Experimental Procedure

During the experiment, there were differences in the steps taken to dry various wet materials. The SCG experiments began by measuring the initial moisture content using laboratory dryer furnaces set to 105℃. The small sample of approximately 1 gram was placed inside the furnace and left for 8 hours to dry completely. After the 8 hours had passed, the initial moisture content was measured using the dried SCG mass. At the same time, 30 g of SCG was left inside the dryer to dewater. Every 2 hours since the beginning of the experiment, new mass measurements were recorded until the mass stopped decreasing. The mass was weighed manually on the weights like in Figure 8. Since the SCG moisture content is dependent on the time spent after it was used to produce a coffee drink, due to it naturally drying in the air, the tried approach was to prepare samples every morning before using them for the experiment. This ensured that the moisture content of the SCG samples was high and that they were approximately equal.

Figure 8. SCG mass measurement

Figure 9. Foam mass measurement

The floral foam drying procedure was mostly similar to drying SCG. However, since the foam was already dry, it needed to be wetted. It was submerged in a container filled with water to obtain a high initial moisture content. It was discovered that reusing the same foam samples was not desirable since the absorbing qualities of the reused sample deteriorated, and it could not reach the initial moisture content that was used previously, meaning that the data from these samples could not be compared to other samples since the moisture content plots would start at different points. Floral foam samples were identically cut into the shape with dimensions (length x width x depth) 6 cm x 6 cm x 1 cm and submerged in room

temperature water for 90 seconds to absorb it. Dry samples weighed about 2 g, but wet samples showed relative dissimilarity, with their weight ranging from 98 g to 151 g. In terms of MC_{wb}, it is a span between 98% and 98.7%, which demonstrates high water absorption capacity.

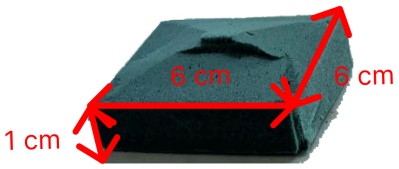

Figure 10. SCG sample dimensions **Figure 11.** Foam sample dimensions

The samples for the experimental part consist of two distinct types: SCG and Foam samples, with specific dimensions for testing in a dryer. The SCG sample has a 6 cm by 6 cm base with a height of 1 cm, while the Foam sample shares the same base dimensions but has a height of 1 cm and features a surface indentation (see Figures 10 & 11). Worth mentioning that due to the material's peculiarities, SCG samples have fillets, while foam has acute edges. Similar geometries were proposed in the simulations to accurately model the real-life characteristics of these materials. The dimensions of the floral foam are designed to imitate the coffee's dimensions, ensuring a more accurate comparison of heat transfer behavior. The difference in their physical characteristics, particularly in texture and surface structure, affected their heat absorption and transfer rates, providing valuable comparable data for the project.

The samples of SCG were obtained from used single-serve coffee containers, also known as coffee pods. The structure of coffee pods is suitable for ensuring the maximum possible similarity of samples, as SCG are tightly placed between two plastic sieves in a plastic container with film on top and a single small through hole for coffee processing. In addition to that, samples were tested within 24 hours of pod usage to guarantee the uniformity of samples. The initial moisture content of the samples was determined by heating three samples from three different pods with an approximate weight of 1 g at 105°C for six hours, until all moisture content was dried. Three moisture contents ranging between 69.4% and

71.3% were obtained, with a mean value of 70.3% being taken as wt% for all coffee samples. Samples placed into the dryer had the identical initial weight of 30 g, using the contents of two coffee pods. Residue was shaped into a whole block with a thickness of about 1 cm.

Two samples of silica gel weighing about 1 g were submerged in water until they changed color from their initial orange to transparent, which indicates that the samples absorbed enough water. When coming into contact with water, in addition to changing the color, silica gel spheres break into fragments with a cracking sound. Change of shape does not affect the absorbing and drying capacity of the material. One of the samples was placed into a dryer while the other was left in an ambient temperature of about 21℃ and relative humidity of 25% while another sample was placed into the dryer. Changes were noticed visually every hour, as when regenerated silica gel gradually changes color back to orange.

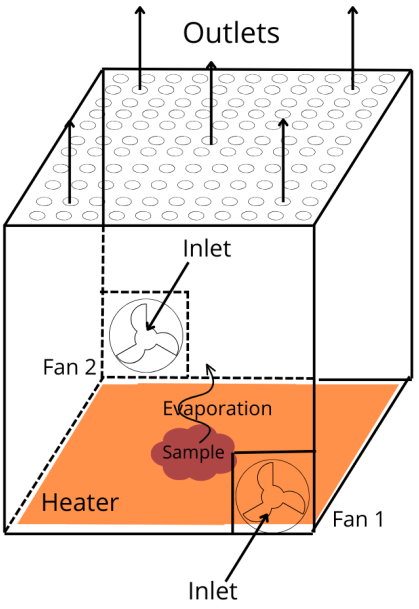

Figure 12. Schematic diagram of the built-forced convection dryer unit with heater

The small-scale dryer unit shown in the schematic diagram (Figure 12) is a built-in forced convection system designed to facilitate the drying process of wet materials. It features 2 inlets and 121 circular outlets at the top for efficient airflow, with fans of 2-watt power capacity that direct air across the sample to promote evaporation of the wet materials. Moreover, the dryer unit is equipped with a heater of 30 watts of power located at the bottom of the dryer below the sample, heating and aiding in the evaporation process, and maintaining the required temperature for drying. Overall, the system is structured to ensure

consistent exposure of the sample to the airflow, optimizing heat transfer and moisture removal during the drying process.

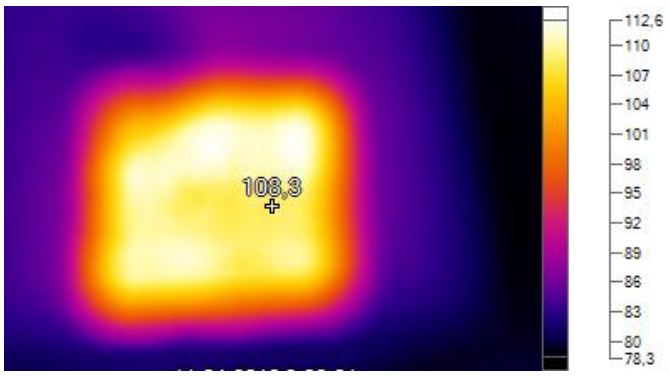

Figure 13. Thermal image of the heater at the bottom of the dryer showing temperature distribution in Fahrenheit during heater on, fans off

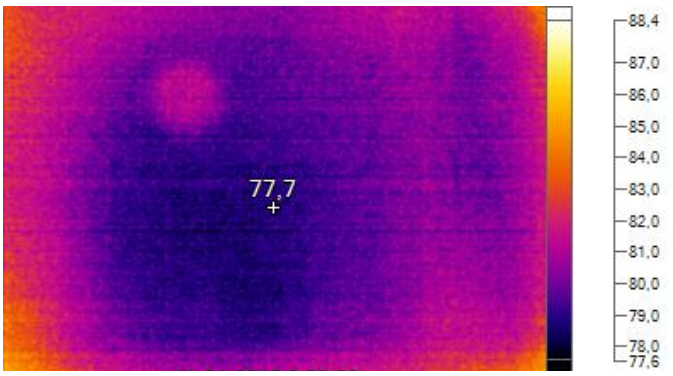

Figure 14. Thermal image of the dryer's bottom of the dryer showing temperature distribution in Fahrenheit during 2 fans on, heater off

The thermal images in Figure 13 and Figure 14 were captured using the *Fluke Thermal Imager Ti 29*, showcasing the heat distribution of a dryer's heater with temperature readings in Fahrenheit. The first image clearly illustrates the varying temperature levels, with the hottest area marked at 108.3°F or 42.4°C, indicating the central point of heat emission. Whereas, in the second picture, where 2 fans are on, the maximum temperature is 77.7°F or 25.4°C. This clearly explains that forced convection did not affect the thermal distribution within the dryer, and room temperature air is circulated without major temperature changes.

The color gradient from purple (25°C) to yellow (45°C) demonstrates the gradual increase in temperature, which is typical for room temperatures. However, one limitation of this thermal analysis is that the heat distribution is non-uniform, meaning that the heat is not evenly

spread across the heater's surface. This can result in areas of higher and lower temperatures, which may affect the efficiency of the heating process and the modeling part.

By incorporating multiple adjustable parameters, such as the control of two fans and a heater, the dryer system offers a wide range of experimental setups, allowing us to manipulate the drying process in various ways. This flexibility ensures that we can test and analyze the impact of each parameter independently or in combination, providing valuable data on how airflow and temperature affect the drying efficiency of the chosen materials. By changing one or more of these parameters, we can observe their contributions to evaporation and heat transfer, which is crucial for optimizing the drying process. Table 1 outlines different experimental conditions and their corresponding setups.

Table 1.
Experimental conditions for drying process

Experiment	**Fan 1**	**Fan 2**	**Heater**
Baseline	*off*	*off*	*off*
Fan 1 on	*on*	*off*	*off*
Heater on	*off*	*off*	*on*
Fan 1 & 2 on	*on*	*on*	*off*
Heater on, fans on	*on*	*on*	*on*

Table 2.
Accuracy and uncertainty of measurement devices

Name of device	**Measured data**	**Range**	**Accuracy**	**Uncertainty**
Electronic balance CAS SW-20	Mass of samples	0.001-20 kg	±0.01 kg	±0.0005 kg
Hygrometer TESTO 610	Relative humidity	0-100%	± 2.5%	± 0.05%
Thermometer TESTO 610	Room temperature	-10˚C to 50˚C	± 0.5˚C	± 0.05˚C

Table 2 presents the accuracy and uncertainty of the main devices used in the study to measure parameters, such as mass, relative humidity, and temperature. It outlines the specifications of the CAS SW-20 electronic balance, the TESTO 610 hygrometer, and the thermometer. Each device is characterized by its specific range, accuracy, and uncertainty, which are crucial for ensuring reliable measurements in the experiment. Worth noting that

one limitation of the CAS SW-20 electronic balance is its potential for inaccurate measurements at very low masses, especially for samples of 30 grams mass, which leads to errors in the mass reading.

3.3 COMSOL simulations

To determine the moisture content through simulations, COMSOL Multiphysics 6.2 was used since it allows one to consider the impact of multiple factors during the drying process. Since the chosen materials display different physical characteristics, SCG being a porous material while the floral foam is more similar to a solid block, different approaches were used to simulate their drying processes.

The model for SCG was created based on the existing official guide on the COMSOL website (*Drying of a Potato Sample*, n.d.). This paper takes into account convection of vapor due to pressure gradient, binary diffusion of water vapor and dry air in a gaseous phase, convection of liquid water due to total pressure gradient, and capillary transport of liquid water to simulate moisture transport within the porous material. It also considers the effect of laminar flow, heat transfer, and permeability of the porous matrix. The same approach used in the paper to simulate the drying process of a potato was used for SCG, the difference being the geometry and the parameters of the material. The geometry was created based on the dimensions of the real dryer, a 30 by 30. The material was placed in the middle of the bottom line of the dryer. Multiple points on the upper line were used to dissect the line to mimic the holes in the cover on top of the dryer. The proportion of the length of these lines that represents the holes was chosen to be the same as the proportion of the holes' area relative to the area of the transparent polymer cover sheet, approximately 40%. The lines on the sides were dissected using another point to use as an inlet representing the fans. The parameters of the SCG were taken from scholarly articles and papers on the material. However, there was a difficulty in finding the physical properties of SCG since the papers used coffee-based products, but not exactly SCG. The porosity, density, and thermal conductivity were approximated based on the study of Ismail et al, who identified a range of values for physical properties of an SCG biocomposite mixed with epoxy resin over varying mixing proportions (2023). Since the values for biocomposite mix are not needed and there is a need for a pure SCG, it was decided to use the 95/5 mix as a percentage of volume, where 95% is SCG volume. The permeability was obtained from the Guerra et al. study that used coffee beds with varying porosity values based on the microscopic structure of the

coffee bed (2022). The study provides a range of permeability values over the porosity axis, where the approximated porosity from the former study was used to obtain the most accurate permeability value. The heat capacity value was obtained from the Telis-Romero et al. paper, which studies the physical properties of a coffee extract (2000). It is comparatively the least accurate measurement since coffee extract is different from SCG. The coffee extract is a liquid substance, while SCG is a solid filled with water. However, due to a lack of studies on the material and the fact that the moisture content of the SCG on the wet basis is high, being 70%, it is a plausible approximation of the real value of the heat capacity of the SCG.

Table 3.
Initial parameters used to develop the simulation in COMSOL

Operating parameters	**Value**	**References**
Ambient temperature, K	298.15	Experimental data
Ambient relative humidity	0.25	Experimental data
Freestream velocity, m/s	3	Computed
Porosity	0.27	(Ismail et al., 2023)
Permeability, m^2	3e-14	(Guerra et al., 2022)
Thermal conductivity, W/(m K)	0.054	(Ismail et al., 2023)
Heat capacity, J/(kg K)	3000	(Telis-Romero et al., 2000)
Density, kg/m^3	500	(Ismail et al., 2023)

Table 3 presents the initial parameters used to develop a simulation in COMSOL Multiphysics 6.2. The parameters include ambient temperature, relative humidity, freestream velocity, porosity, and others. Some of these parameters were taken from the literature review, while some were taken directly from experiments or computed, ensuring the model is based on reliable and relevant information. They are essential to simulate the material's mechanical properties and accurately model the system's behavior.

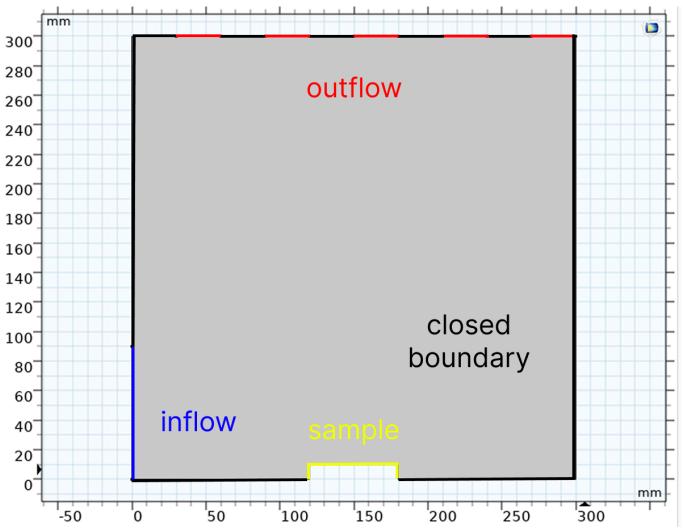

Figure 15. Geometric configuration of the 2D model with boundary conditions

Figure 15 depicts the geometric configuration of the 2D model. Their uniform properties were assumed along the Z-axis. The model comprises one square domain – a 30 by 30 cm dryer, one rectangular material sample of 1 by 6 cm. Red lines on the top represent outflow; blue lines represent forced convective inflow; yellow lines - material sample boundaries; all black lines represent the wall and closed boundary. The geometry for the perforated roof of the dryer creates an open area of 50%, as in the 3D experimental dryer.

3.4 Economic aspect

The global adoption of solar dryers has been driven by the increasing demand for sustainable and energy-efficient drying technologies (Pirasteh et al., 2014). When breaking down the economic aspect of utilizing the proposed dryer design, total costs are made up of capital costs of materials and manufacturing, and costs of dryer operation. Heating system based on evacuated tube collectors costs more than conservative electric heating elements, such as polyimide heating plates. However, this difference in costs is compensated by lower maintenance costs of evacuated tube systems, significantly less electricity consumption, and the possibility to fund drying units and related infrastructure by state subsidies for energy-efficient projects (Kachalova, 2023).

4 Results

4.1 CFD Simulations

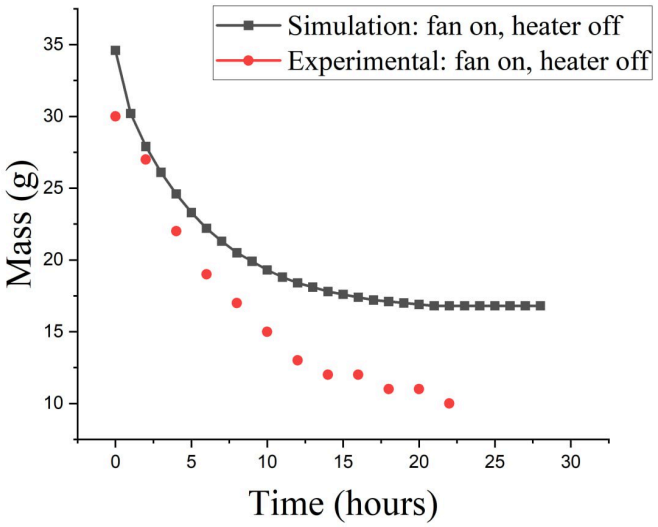

Figure 16. Simulation vs Experiment: SCG, fan on, heater off

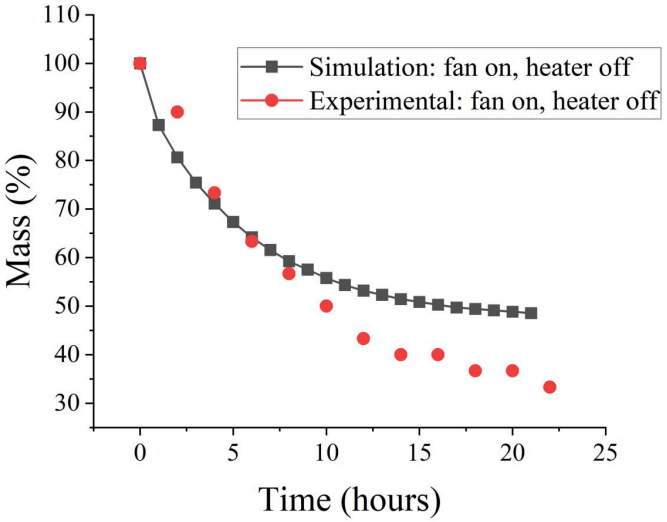

Figure 17. Simulation vs Experiment in terms of mass fraction

The results obtained from COMSOL diverge from the experimental results. To start, the initial mass of the simulated SCG is 34.6 g compared to the 30 g in the experiment. This could be explained by the fact that the initial parameters were approximated due to a lack of research on the material. Figure 17 tries to account for that and compares the experimental and simulated results in terms of the mass percentage. This way, both results start at 100% of mass, and the drying behavior could be directly compared. However, even in this case, the

experimental results exhibit a significantly faster drying behavior. This is evident from the fact that the simulation curve levels at approximately 50%, while the experimental results dip to around 30%. This could be partially explained by the fact that, supposedly, in the real dryer, the creation of helical air movement drives the drying rate, while it is non-existent in the 2D simulation of the dryer.

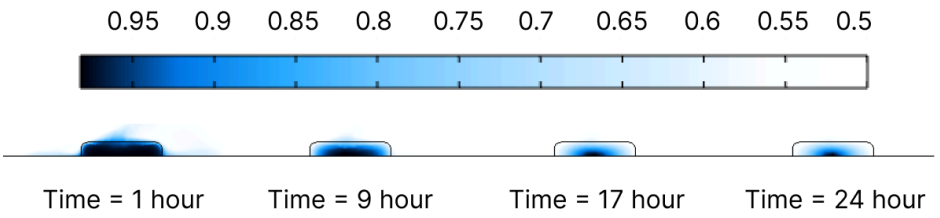

Figure 18. Relative humidity of SCG over time

Figure 18 shows the change in relative humidity of the SCG porous medium over time. In the beginning, the relative humidity has a high value since it is completely wet. As time passes, the relative humidity on the boundaries of the medium drops, which can be seen at 9 and 17 hours. After 24 hours have passed, the relative humidity value is high only in the bottom middle part of the medium, and the boundaries are completely white, indicating a relative humidity of 0.5

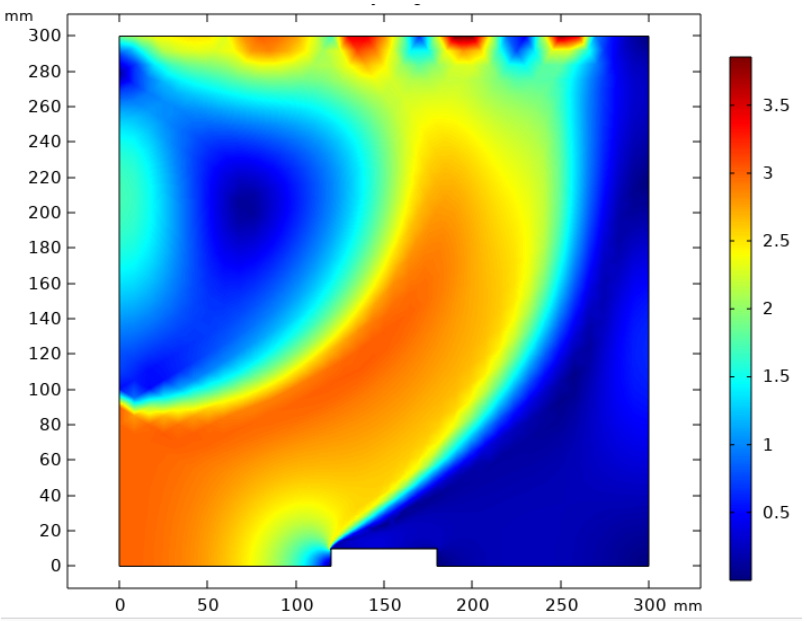

Figure 19. Freestream profile of floral foam (m/s)

Figure 19 displays the velocity profile inside the dryer when simulating the floral foam. The figure shows that as the airflow enters through the fan on the bottom left of the plot, it moves upwards. At the same time, the airflow is slow at the back of the foam, indicating that the floral foam is acting as an obstacle and is not letting the airflow pass through. The airflow speed is high at the outlets of the dryer and slow between the outlets, which is also something to be expected, since the airflow is stopped by the wall that is located there.

4.2 Dryer Experiments

Table 3. SCG, two fans, heater on configuration

Material	SCG		
Configuration	Two fans, heater on		
Time (h)	Mass (g)	MC_{wb} (%)	Drying Rate (g_{wet}/g_{total} h)
0	30	70.3	5.4
2	22	59.5	5.96
4	17	47.6	8.06
6	13	31.5	2.86
8	12	25.8	3.38
10	11	19	4.05
12	10	10.9	4.95
14	9	1	0
16	9	1	0
18	9	1	0
20	9	1	0
22	9	1	0

Table 3 shows the measurement of mass over time. The tables of other experiments with other configurations and/or materials are located in the Appendix. Moisture content on a wet basis and drying rate values were calculated based on the mass of the sample at given times using Formulas 1 and 2.

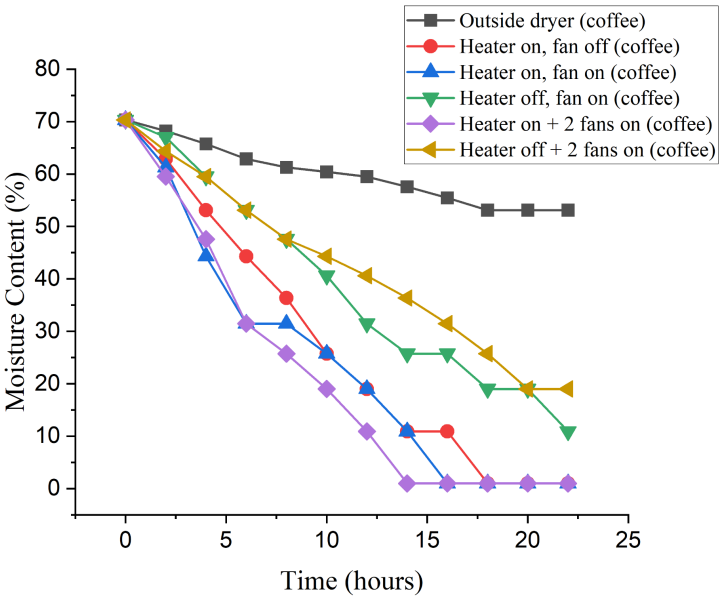

Figure 20. Moisture content on a wet basis of SCG over time

The downscaled drying unit showed drying capability and its effectiveness. Figure 20 shows that the drying unit could dry SCG in 13-16 hours, eliminating half of the moisture inside the residue in 5-8 hours. In contrast to ambient temperature drying, which had little to no effect (from 70.3% to 53.1% in 22 hours), the drying unit successfully managed to dry the material in 14 hours with both fans and the heater, and 18 hours with only the heating film working. Experiments also demonstrated that the effect of the heater is greater than the effect of fans, as a dryer with a heating element only is capable of total drying within 22 hours, which was not detected in the “fan only” setup (10.9% at the 22-hour mark).

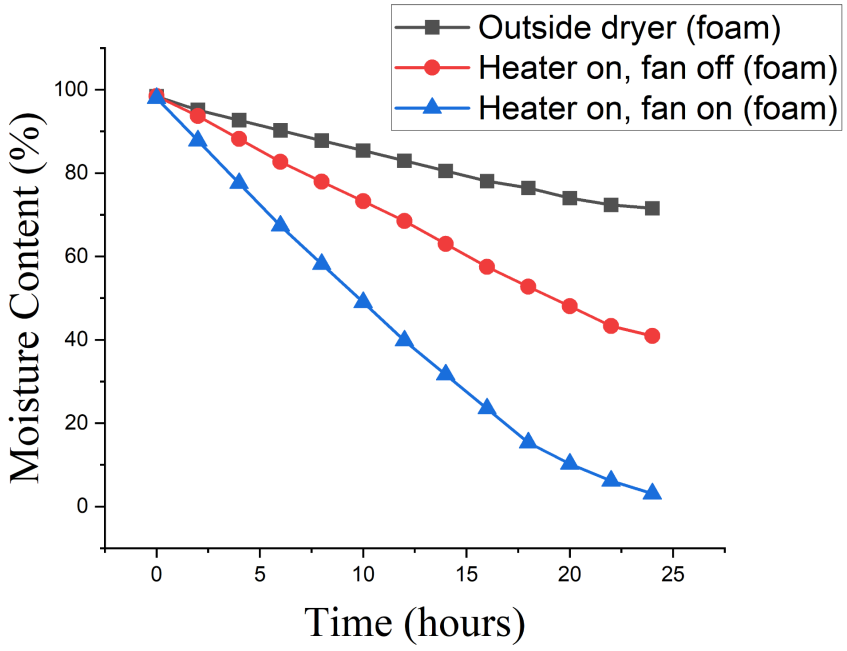

Figure 21. Moisture content on a wet basis of floral foam over time

Results of drying floral foam are presented in Figure 21. The most noticeable takeaway from experiments with floral foam is the almost linear drying rate for this type of material. Regardless of the drying setup, the mass of evaporated fluid stayed constant for the first 16 hours of the experiment. Unlike SCG, where most intensive drying took place in the first 4-6 hours, floral foam showed a constant drying rate for almost the whole span of the experiment. This could be explained by the fact that no material structure took place during the drying of the floral foam. SCG changed its consistency from a wet, paste-like substance with lumps to a totally dry powder resembling sand. In contrast, floral foam stayed the same structurally, as water was only filling cavities inside the foam and leaving the foam block unchanged from a structural point of view. Overall, as Figure 21 demonstrates, the dryer has high drying capabilities. Similar to SCG experiments, ambient temperature drying showed little to no effect (from 98.4% to 71.6% in 24 hours). In the same period, the dryer with only a heating element showed a drop from 98.5% to 40.9%. Most importantly, the dryer with both fan and heating element was capable of almost completely drying the floral foam sample (from 98% down to 1.8%). This is a clear illustration of the importance of fans for drying more uniform materials without phase change.

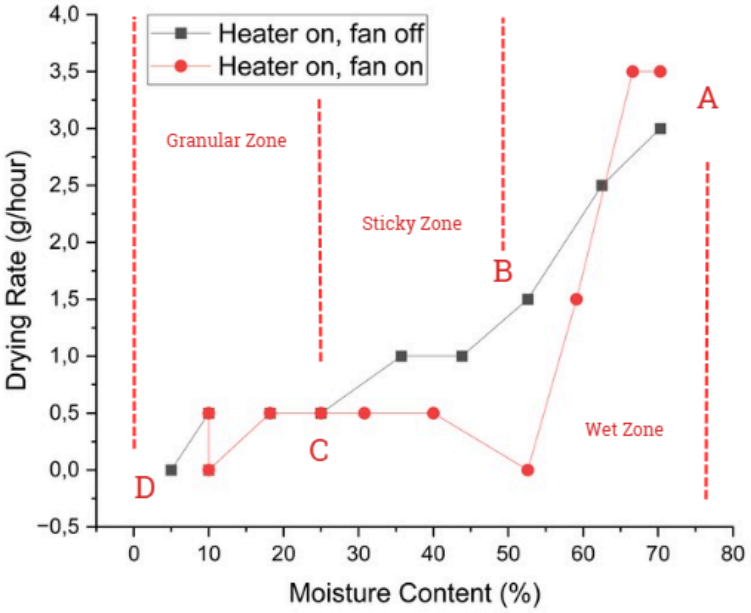

Figure 22. Drying Curve

According to An-nori (2022), the drying process consists of several phases. It begins with a constant drying rate, followed by two periods of decreasing rates, during which water is progressively removed from the material. First as interstitial water, then as surface water. Ultimately, the equilibrium stage is reached, where only bound water remains, which is chemically bonded to the material and can only be eliminated using thermal energy. Figure 22 depicts the drying curve of a sample in the experiment, where the drying curve was the most representative. It illustrates how the drying rate changes as the moisture content decreases. Initially (at point A), the sample has the highest moisture content, dominated by free water. As the drying goes on, there is a sharp decline in moisture content to point B, as interstitial water starts to be removed. In the second falling rate period (point C), the sample becomes more easily mixable, signifying the removal of surface water. Finally, at point D, the equilibrium stage is reached.

In the beginning material goes through a wet zone with high moisture content. After that material switches to the sticky zone with 20-50% moisture content. The material becomes pasty, reducing the drying rate as interstitial water is removed. Finally, the granular zone is reached. It is characterized by a low but steady drying rate as surface water is gradually removed in this zone.

Figure 23. Dry silica gel sample

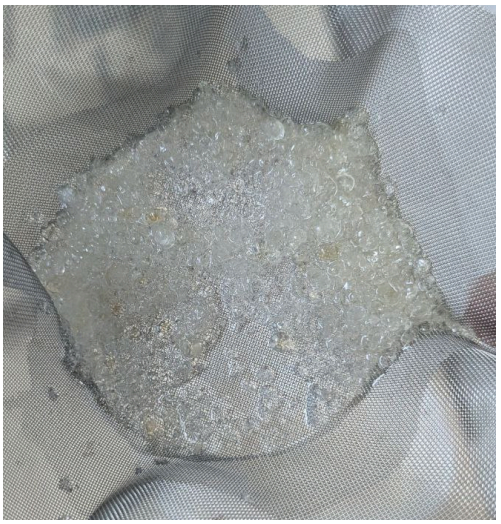

Figure 24. Soaked silica gel sample

Figure 25. Silica gel sample after 5 hours in the dryer

Figure 23 depicts the initial condition of dry silica gel as orange spheres. After fully submerging the metal mesh with silica gel, cracking sounds started appearing. As Figure 24 shows, it was a sign of silica gel spheres breaking into smaller fragments after soaking the maximum possible amount of water. After placing the sample in the dryer for 5 hours with both fans and the heater working, most of the silica gel started regaining its orange color, indicating its regeneration as the moisture content decreased (Figure 25). This not only shows drying capabilities of the dryer that are applicable for silica gel but also proves a study by Pramuang and Exell (2004), showing that silica gel regeneration is very much possible at lower temperatures of approximately 40℃.

5 Analysis and Discussions

Experimental results showed that drying of wet materials without using high heat input and sharp temperature gradients is possible and efficient. By graphically presenting results and comparing baseline case scenarios with designed ones, efficiency was proven. A configuration with two fans could be used as a partial substitution for the heater. This configuration does not necessarily achieve the same result in terms of drying, but it is not that significant considering the fact that it consumes a significantly smaller amount of energy. Even better drying capacity was observed when using both the heater and two fans. The highest initial drying rate and fastest time to dry were observed using this configuration. However, several limitations were present while conducting the experiments. First of all, there are concerns regarding the precision of weights. As they displayed mass rounded to the closest gram, it was problematic to show data at final stages of drying, as moisture content changes were smaller than 1 g for longer than two hours; therefore calculated drying rate was zero even though drying took place. Low accuracy of weights was not that impactful during floral foam experiments, as it gave an error of ±1% for samples weighing around 100 g, but was more noticeable for coffee samples and was the reason why no numerical data for silica gel samples were gained.

Another problem encountered during the experiments was the specifics of working with floral foam. It should be noted that working with floral foam requires additional safety measures, as microparticles of floral foam can irritate the breathing organs and eyes. In addition to that, floral foam itself is not an environmentally friendly material. Therefore, the experimental procedure of this research is not necessarily environmentally friendly, even though all of the floral foam used in experiments was discarded for plastic recycling. For future research, using more sustainable materials would be a preferable choice.

One of the limitations of this dryer is the reliance on weather conditions. The experiments were conducted over the span of 2 months, during which the winter had ended, and the humidity both indoors and outdoors considerably increased. This could be verified using online databases that store weather conditions information or measured directly, which we did. The readings for the indoor relative humidity were 25% at the beginning of March and around 45% at the end of April. Most likely, this fact had a negative effect on the results of experiments with two fans, since the results show that among configurations without a heater and using only one fan is better than using two fans.

Overall, the results show that using fans seems to improve the drying rate of at least floral foam. However, the results of the SCG experiments are inconclusive. While the two fans with a heater configuration was the one with the fastest drying time, the two fans without a heater configuration was drastically worse in terms of drying rate. This might be due to the material type difference and the fact that SCG is a porous material, while floral foam is not. This is also reflected in the plots of both materials. The SCG samples displayed exponential decay, while the floral foam had a mostly linear decay with a slight leveling off at the end. To make a more accurate statement, more data with other types of material is needed since even the SCG has relatively low porosity, which depends on the pressure it underwent inside the coffee machine.

6 Conclusion

In this project, a design for a drying unit that utilizes the low humidity of the environment was suggested. To provide ground for dryer design, the requirements of industry as well as previous findings on this topic were investigated. Viability and efficiency of the suggested design were tested both experimentally and analytically via a numerical approach in COMSOL software, and both test results were compared to validate the design choice. Materials targeted for drying were spent coffee grounds, floral foam, and silica gel, chosen based on industry demand and/or specific material properties. All experiments showed that the dryer fulfills its drying requirements, as it successfully dried both 30 g samples of SCG with a wt% of 70% and 100 g samples of wet floral foam with a wt% of 98% within 20-24 hours. Experiments with silica gel proved the viability of a non-traditional approach of silica gel regeneration, as drying of silica gel was achieved at much lower temperatures (about 40℃) thanks to air flow.

7 Appendix

Table 4. SCG, no fans, heater off configuration

Material	SCG		
Configuration	No fans, heater off		
Time (h)	Mass (g)	MC_{wb} (%)	Drying Rate (g_{wet}/g_{total} h)
0	30	70.3	1.06
2	28	68.2	1.22
4	26	65.7	1.43
6	24	62.9	0.81
8	23	61.3	0.43
10	22.5	60.4	0.45
12	22	59.5	0.96
14	21	57.6	1.06
16	20	55.5	1.17
18	19	53.1	0
20	19	53.1	0
22	19	53.1	0

Table 5. SCG, no fans, heater on configuration

Material	SCG		
Configuration	No fans, heater on		
Time (h)	Mass (g)	MC_{wb} (%)	Drying Rate (g_{wet}/g_{total} h)
0	30	70.3	3.71
2	24	62.9	4.88
4	19	53.1	4.40
6	16	44.3	3.98
8	14	36.4	5.30
10	12	25.8	3.38

12	11	19.0	4.05
14	10	10.9	0
16	10	10.9	4.95
18	9	1.0	0
20	9	1.0	0
22	9	1.0	0

Table 6. SCG, one fan, heater off configuration

Material	SCG		
Configuration	One fan, heater off		
Time (h)	Mass (g)	MC_{wb} (%)	Drying Rate (g_{wet}/g_{total} h)
0	30	70.3	1.65
2	27	67	3.75
4	22	59.5	3.20
6	19	53.1	2.76
8	17	47.6	3.49
10	15	40.6	4.57
12	13	31.5	2.86
14	12	25.8	0
16	12	25.8	3.38
18	11	19	0
20	11	19	4.05
22	10	10.9	0

Table 7. SCG, one fan, heater on configuration

Material	SCG
Configuration	One fan, heater on

Time (h)	Mass (g)	MC_{wb} (%)	Drying Rate (g_{wet}/g_{total} h)
0	30	70.3	4.52
2	23	61.3	8.47
4	16	44.3	6.43
6	13	31.5	0
8	13	31.5	2.86
10	12	25.75	3.38
12	11	19	4.05
14	10	10.9	4.95
16	9	1	0
18	9	1	0
20	9	1	0
22	9	1	0

Table 8. SCG, two fans, heater off configuration

Material	SCG		
Configuration	Two fans, heater off		
Time (h)	Mass (g)	MC_{wb} (%)	Drying Rate (g_{wet}/g_{total} h)
0	30	70.3	2.97
2	25	64.36	2.43
4	22	59.5	3.197368421
6	19	53.1	2.758513932
8	17	47.6	1.637867647
10	16	44.3	1.85625
12	15	40.6	2.121428571
14	14	36.6	2.447802198
16	13	31.5	2.855769231

18	12	25.8	3.375
20	11	19	0
22	11	19	0

Table 9. Floral foam, no fans, heater off configuration

Material	Floral foam		
Configuration	No fans, heater off		
Time (h)	Mass (g)	MC_{wb} (%)	Drying Rate (g/h)
0	123	98.4	1.63
2	119	95.1	1.22
4	116	92.7	1.22
6	113	90.2	1.22
8	110	87.8	1.22
10	107	85.4	1.22
12	104	82.9	1.22
14	101	80.5	1.22
16	98	78.0	0.81
18	96	76.4	1.22
20	93	74.0	0.81
22	91	72.4	0.41
24	90	71.5	0

Table 10. Floral foam, no fans, heater on configuration

Material	Floral foam		
Configuration	No fans, heater on		
Time (h)	Mass (g)	MC_{wb} (%)	Drying Rate (g/h)
0	127	98.4	2.36

2	121	93.7	2.76
4	114	88.2	2.76
6	107	82.7	2.36
8	101	78.0	2.36
10	95	73.2	2.36
12	89	68.5	2.76
14	82	63.0	2.76
16	75	57.5	2.36
18	69	52.8	2.36
20	63	48.0	2.36
22	57	43.3	1.18
24	54	40.9	0

Table 11. Floral foam, one fan, heater on configuration

Material	Floral foam		
Configuration	One fan, heater on		
Time (h)	Mass (g)	MC_{wb} (%)	Drying Rate (g/h)
0	110	98.2	5.45
2	98	87.3	5.45
4	86	76.4	5
6	75	66.4	4.54
8	65	57.3	5
10	54	47.3	3.64
12	46	40	5.45
14	34	29.1	3.64
16	26	21.8	3.64
18	18	14.5	2.73

20	12	9.1	2.23
22	7	4.5	1.36
24	4	1.8	0

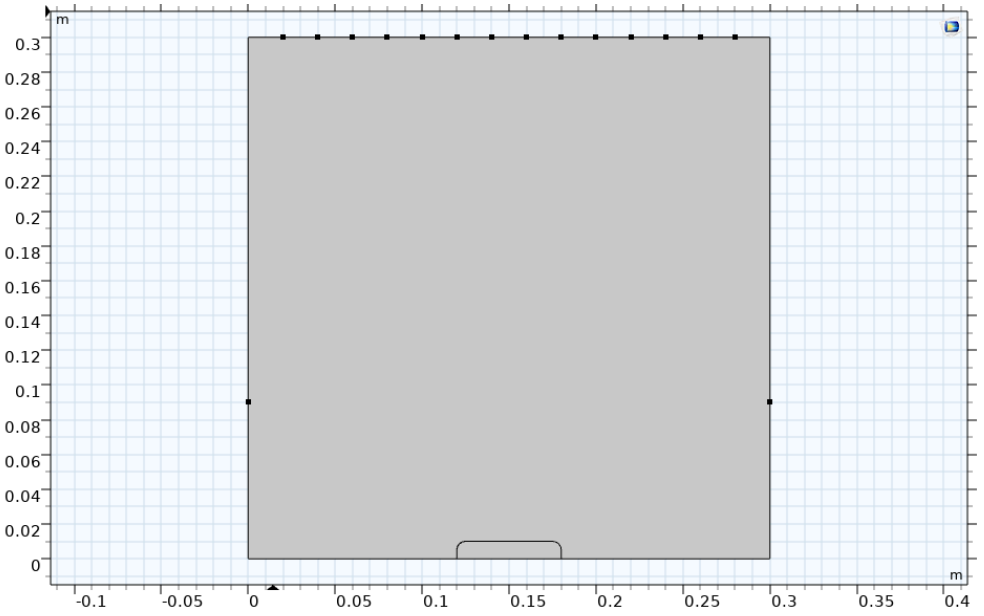

Figure 26. 2D geometry of the dryer

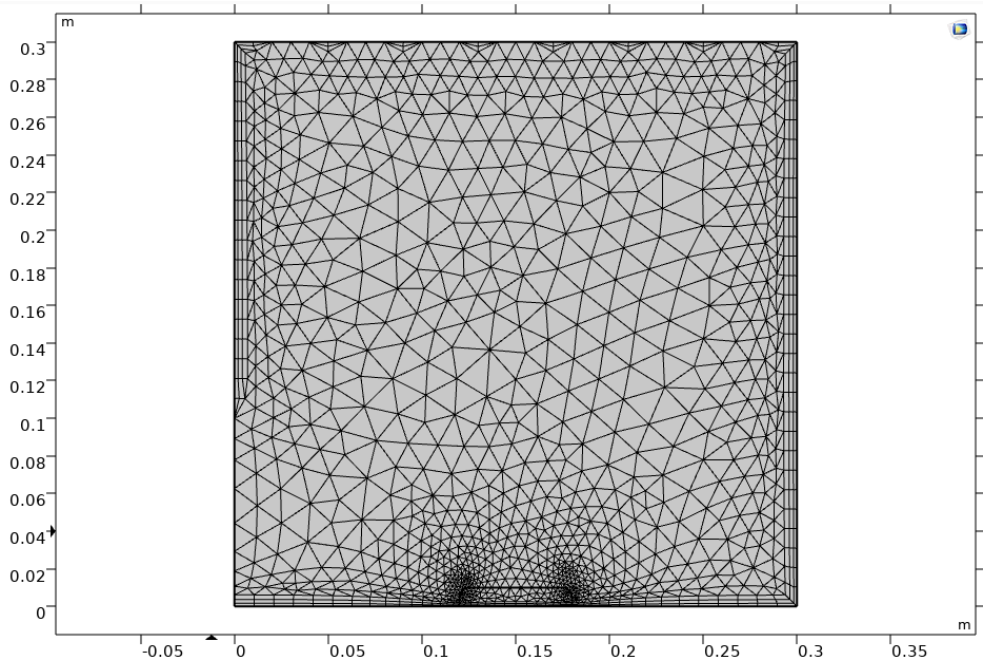

Figure 27. Mesh of the SCG simulation model

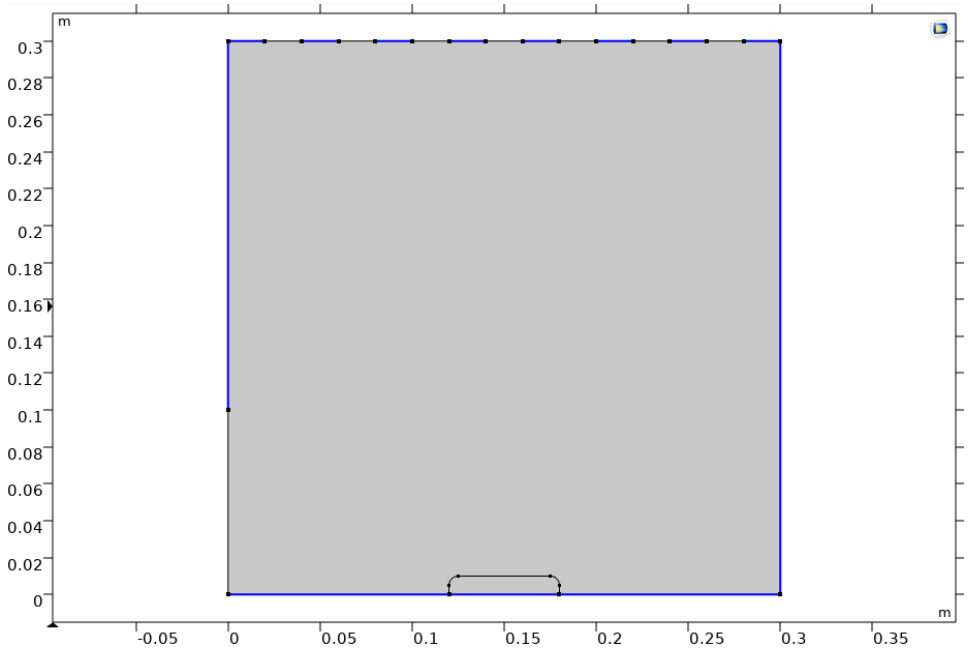

Figure 28. Walls of the SCG simulation model

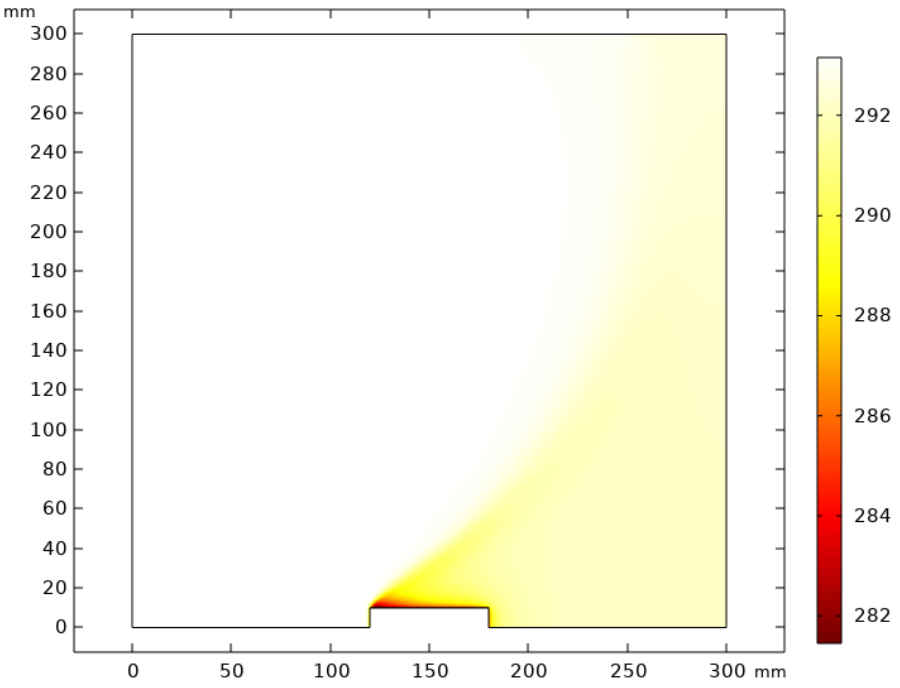

Figure 29. Temperature: floral foam [K]

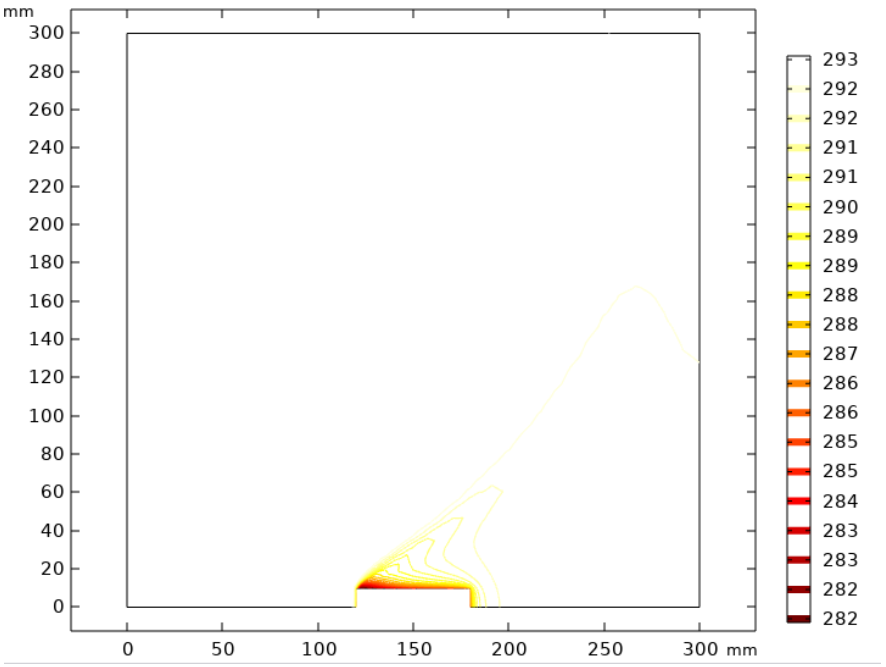

Figure 30. Isothermal contours: floral foam [K]

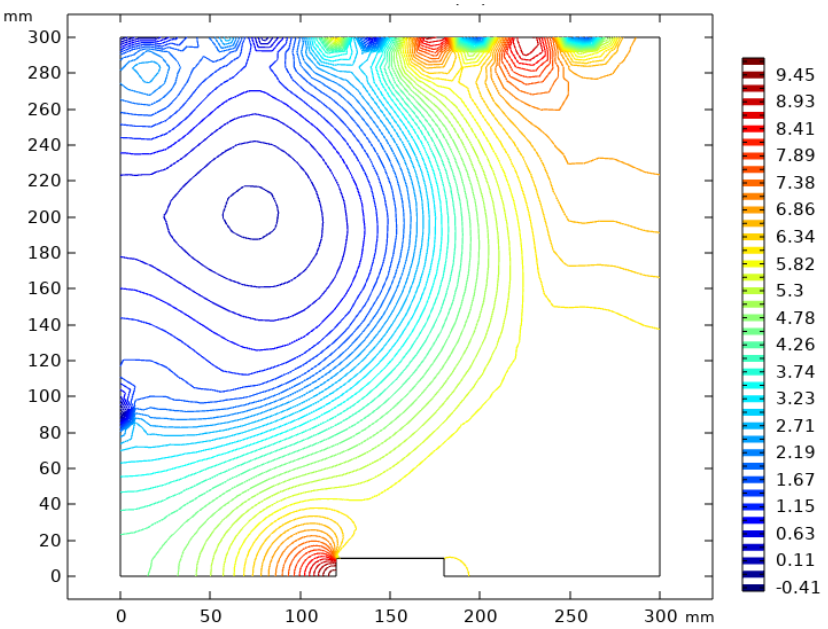

Figure 31. Surface: velocity magnitude: floral foam (m/s)

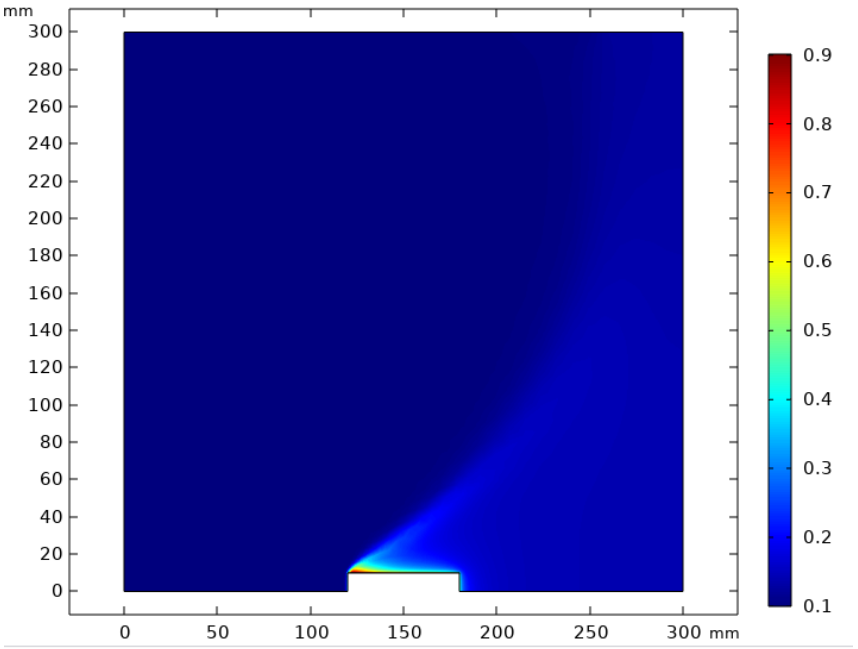

Figure 32. Surface: relative humidity: floral foam

8 References

Ameri, B., Hanini, S., & Boumahdi, M. (2019). Influence of drying methods on the thermodynamic parameters, effective moisture diffusion and drying rate of wastewater sewage sludge. *Renewable Energy*, *147*, 1107–1119. https://doi.org/10.1016/j.renene.2019.09.072

An-Nori, A., Ezzariai, A., Mejahed, K. E., Fels, L. E., Gharous, M. E., & Hafidi, M. (2022). Solar Drying as an Eco-Friendly Technology for sewage sludge Stabilization: Assessment of micropollutant behavior, pathogen removal, and agronomic value. Frontiers in Environmental Science, 10. https://doi.org/10.3389/fenvs.2022.814590

Belloulid, M. O., Hamdi, H., Mandi, L., & Ouazzani, N. (2019). Solar drying of wastewater sludge: a case study in Marrakesh, Morocco. Environmental technology, 40(10), 1316-1322.

Bennamoun L.; Leonard A. Etude experimentale et modelisation du sechage des boues generees parl'epuration des eaux usees. Revue des Energies Renouvelables (2011), 14: 1-12.

Carrasco, M., & Gao, W. (2019). Sludge Particle Size and Correlation with Soluble Organic Matter and Conditioning Characteristics After Freezing Treatments. *Water Air & Soil Pollution*, *230*(3). https://doi.org/10.1007/s11270-019-4107-z

Drying of a potato sample. (n.d.). COMSOL. https://www.comsol.com/model/drying-of-a-potato-sample-102411

DSouza, G.C., Li, H., Yuan, Z., Xum, C.C., Ray, M.B. (2022). Investigating the hydrophilicity of phenol formaldehyde foams: Effects of synthesis parameters. https://doi.org/10.1002/app.54877

Ejeian, M., & Wang, R. (2021). Adsorption-based atmospheric water harvesting. *Joule*, *5*(7), 1678–1703. https://doi.org/10.1016/j.joule.2021.04.005

Ekechukwu, O. V. (1999). Review of solar-energy drying systems I: an overview of drying principles and theory. Energy conversion and management, 40(6), 593-613.

Goh, L. J., Othman, M. Y., Mat, S., Ruslan, H., & Sopian, K. (2011). Review of heat pump systems for drying application. *Renewable and Sustainable Energy Reviews*, *15*(9), 4788–4796. https://doi.org/10.1016/j.rser.2011.07.072

Guerra, M. V., Harshe, Y. M., Fries, L., Rothberg, S., Palzer, S., & Heinrich, S. (2022). Influence of particle size distribution on espresso extraction via packed bed compression. *Journal of Food Engineering*, *340*, 111301. https://doi.org/10.1016/j.jfoodeng.2022.111301

Hebbar, H., Vishwanathan, K., & Ramesh, M. (2004). Development of combined infrared and hot air dryer for vegetables. *Journal of Food Engineering*, *65*(4), 557–563. https://doi.org/10.1016/j.jfoodeng.2004.02.020

Hu, Y., & Wang, Y. (2016). Study on the dewatering process for water treatment residuals: Applicability of freezing–thawing, compression, and electro-osmotic treatment. *Drying Technology*, *35*(12), 1450–1459. https://doi.org/10.1080/07373937.2016.1253021

Ibrahim, A., Amer, A., Elsebaee, I., Sabahe, A., & Amer, M. A. (2024). Applied insight: studying reducing the carbon footprint of the drying process and its environmental impact and financial return. Frontiers in Bioengineering and Biotechnology, 12. https://doi.org/10.3389/fbioe.2024.1355133

International Energy Agency. (2022). Kazakhstan - countries & regions. IEA. https://www.iea.org/countries/kazakhstan/coal

Ismail, I., Aini, Q., Maulida, C. R., Mursal, N., Jalil, Z., & Fadzullah, S. H. S. M. (2023). Thermal properties of spent coffee ground biocomposite using epoxy resin matrix. AIP Conference Proceedings, 2613, 020009. https://doi.org/10.1063/5.0119827

Kachalova, N. (2023). Kak v Kazahstane stimuliruyut vnedrenie energoeffektivnyh

tehnologij [How integration of energy-effective technologies is being stimulated in Kazakhstan]. *Kursiv*. https://kz.kursiv.media/2023-03-31/kak-v-kazahstane-stimuliruyut-vnedrenie-energoeffektivnyh-tehnologij/

Kamarulzaman, A., Hasanuzzaman, M., & Rahim, N. (2021). Global advancement of solar drying technologies and its future prospects: A review. *Solar Energy*, *221*, 559–582. https://doi.org/10.1016/j.solener.2021.04.056

Karamanis, K.. (2015). Eco-Efficient Materials for Mitigating Building Cooling Needs. https://doi.org/10.1016/B978-1-78242-380-5.00010-8

Kourmentza, C., Economou, Ch.N., Tsafrakidou, P., Kornaros, M. (2018). Spent coffee grounds make much more than waste: Exploring recent advances and future exploitation strategies for the valorization of an emerging food waste stream. https://doi.org/10.1016/j.jclepro.2017.10.088

Kumar, L., Hasanuzzaman, M., & Rahim, N. (2019). Global advancement of solar thermal energy technologies for industrial process heat and its future prospects: A review. *Energy Conversion and Management*, *195*, 885–908. https://doi.org/10.1016/j.enconman.2019.05.081

Kumar, M., Sansaniwal, S. K., & Khatak, P. (2015). Progress in solar dryers for drying various commodities. *Renewable and Sustainable Energy Reviews*, *55*, 346–360. https://doi.org/10.1016/j.rser.2015.10.158

Lima, M. R. P., Zandonade, E., & Sobrinho, P. A. (2012). Characteristics of WWTP sludge after drying in greenhouse for agricultural purposes. Water Science and Technology, 66(7), 1460-1466.

Liu, X., Huang, X., Wu, Y., Xu, Q., Du, M., Wang, D., Yang, Q., Liu, Y., Ni, B., Yang, G., Yang, F., & Wang, Q. (2020). Activation of nitrite by freezing process for anaerobic

digestion enhancement of waste activated sludge: Performance and mechanisms. *Chemical Engineering Journal*, *387*, 124147. https://doi.org/10.1016/j.cej.2020.124147

Markova, A. (2025, February 17). Kazakhstan's coffee craze gets pricey. *Kursiv.* https://kz.kursiv.media/en/2025-02-17/engk-yeri-kazakhstans-coffee-craze-gets-pricey-espresso-costs-up-16/

Mevada, D., Panchal, H., ElDinBastawissi, H. A., Elkelawy, M., Sadashivuni, K., Ponnamma, D., ... & Sharshir, S. W. (2022). Applications of evacuated tubes collector to harness the solar energy: a review. International Journal of Ambient Energy, 43(1), 344-361.

Mujumdar, A. S., & Devahastin, S. (2000). Fundamental principles of drying. *Exergex, Brossard, Canada*, *1*(1), 1-22. https://www.academia.edu/download/32365386/Drying.pdf

Mujumdar, A. S. (2015). Handbook of industrial drying (4th ed.). CRC Press.

Musembi, M. N., Kiptoo, K. S., & Yuichi, N. (2016). Design and analysis of solar dryer for Mid-Latitude Region. *Energy Procedia*, *100*, 98–110. https://doi.org/10.1016/j.egypro.2016.10.145

Nyssanbayeva, A. S., Cherednichenko, A. V., Cherednichenko, V. S., Abayev, N. N., & Madibekov, A. S. (2019). Bioclimatic conditions of the winter months in Western Kazakhstan and their dynamics in relation to climate change. International journal of biometeorology, 63, 659-669.

Pakari, A., & Ghani, S. (2019). Airflow assessment in a naturally ventilated greenhouse equipped with wind towers: Numerical simulation and wind tunnel experiments. Energy and Buildings, 199, 1-11.

Pandey, S., Kumar, A., & Sharma, A. (2024). Sustainable solar drying: Recent advances in materials, innovative designs, mathematical modeling, and energy storage solutions.

Energy, 132725.

Parker, P. J., & Collins, A. G. (1998). Dehydration of flocs by freezing. *Environmental Science & Technology*, *33*(3), 482–488. https://doi.org/10.1021/es980705p

Pikoń, J. (1995). Drying of coal. Handbook of Industrial Drying, Revised and Expanded, 2, 977.

Pirasteh, G., Saidur, R., Rahman, S. M. A., & Rahim, N. A. (2014). A review on development of solar drying applications. Renewable and Sustainable Energy Reviews, 31, 133–148. doi:10.1016/j.rser.2013.11.052

Ratti, C. (2001). Hot air and freeze-drying of high-value foods: a review. https://doi.org/10.1016/S0260-8774(00)00228-4

Salihoglu N. K.; Pinarli V.; Salihoglu G. Solar drying in sludge management in Turkey. Renewable Energy (2007), 32: 1661-1675.

Schneid, S., Cohrs, M., Lenger, J. (2025). Scaling up controlled nucleation in freeze drying: Translating vacuum-induced surface freezing from laboratory to GMP. https://doi.org/10.1016/j.ejps.2024.106968

Sharma, K., Kothari, S., Panwar, N., & Patel, M. R. (2022). Influences of a Novel Cylindrical Solar Dryer on Farmer's Income and its Impact on Environment. *Research Square (Research Square)*. https://doi.org/10.21203/rs.3.rs-1477039/v1

Sivakumar, R., Saravanan, R., Perumal, A. E., & Iniyan, S. (2016). Fluidized bed drying of some agro products – A review. Renewable and Sustainable Energy Reviews, 61, 280–301. https://doi.org/10.1016/j.rser.2016.04.014

Spotar, S. Y., Moldabek, M. O., & Baitemir, A. B. (2020, September 12). VORTEX DEHYDRATOR FOR APPLE SNACKS. https://www.scientific-publications.net/en/article/1002015/

Stream Peak International. (2023). Everything You Need To Know About Silica Gel.

https://www.streampeakgroup.com/everything-you-need-to-know-about-silica-gel/#:~:text=The%20most%20common%20methods%20for,for%20approximately%201%2D2%20hours

Telis‐Romero, J., Gabas, A. L., Polizelli, M. A., & Telis, V. R. N. (2000). Temperature and water content influence on thermophysical properties of coffee extract. International Journal of Food Properties, 3(3), 375–384. https://doi.org/10.1080/10942910009524642

Wang, W., Li, M., Hassanien, R. H. E., Wang, Y., & Yang, L. (2018). Thermal performance of indirect forced convection solar dryer and kinetics analysis of mango. *Applied Thermal Engineering*, *134*, 310–321. https://doi.org/10.1016/j.applthermaleng.2018.01.115

Wang, Y., Lu, S., Ren, T., & Li, B. (2011). Bound water content of Air‐Dry soils measured by thermal analysis. *Soil Science Society of America Journal*, *75*(2), 481–487. https://doi.org/10.2136/sssaj2010.00

wet basis. (n.d.). https://engineering.purdue.edu/~abe305/moisture/html/page8.htm

Wu, Y., Gao, M., Zhang, X., Zhang, Y., & Ji, J. (2023). Effect of initial water content on the dewatering performance of freeze-thaw preconditioned landfill sludge. *Environmental Research*, *239*, 117356. https://doi.org/10.1016/j.envres.2023.117356

Yin, L., Guo, Y., Wang, Z., Shan, Y., Duan, P., & Wang, C. (2023). Steam explosion coupled with freeze-thaw cycles: An efficient and environmentally friendly method for deep dewatering of sewage sludge. *Journal of Water Process Engineering*, *51*, 103462. https://doi.org/10.1016/j.jwpe.2022.103462

Zheleznova, I., Gushchina, D., Meiramov, Z., & Olchev, A. (2022). Temporal and Spatial Variability of Dryness Conditions in Kazakhstan during 1979–2021 Based on Reanalysis Data. *Climate*, *10*(10), 144. https://doi.org/10.3390/cli10100144

Климат Астаны - Погода и климат. (n.d.). http://www.pogodaiklimat.ru/climate/35188.htm